



An electrochemical biosensor for determination of hydrogen peroxide using nanocomposite of poly(methylene blue) and FAD hybrid film

Kuo-Chiang Lin, Chien-Yu Yin, Shen-Ming Chen*

Electroanalysis and Bioelectrochemistry Lab, Department of Chemical Engineering and Biotechnology, National Taipei University of Technology, No.1, Section 3, Chung-Hsiao East Road, Taipei 106, Taiwan, ROC

ARTICLE INFO

Article history:

Received 17 December 2010
Received in revised form 12 February 2011
Accepted 22 March 2011
Available online 31 March 2011

Keywords:

Hydrogen peroxide
FAD
Methylene blue
NADH

ABSTRACT

An electrochemical biosensor for determination of hydrogen peroxide (H_2O_2) has been developed by the hybrid film of poly(methylene blue) and FAD (PMB/FAD). The PMB/FAD hybrid film was performed in PBS (pH 7) containing methylene blue and FAD by cyclic voltammetry. Repeatedly scanning potential range of -0.6 – 1.1 V, FAD was immobilized on the electrode surface by electrostatic interaction while methylene blue was electropolymerized on electrode surface. This modified electrode was found surface confined and pH dependence. It showed good electrocatalytic reduction for H_2O_2 , KBrO_3 , KIO_3 , and NaClO as well as electrocatalytic oxidation for NADH. At an applied potential of -0.45 V vs. Ag/AgCl, the sensor showed a rapid and linear response to H_2O_2 over the range from 0.1 μM to 960 μM , with a detection limit of 0.1 μM and a significant sensitivity of 1109 $\mu\text{A mM}^{-1} \text{cm}^{-2}$ ($S/N=3$). It presented excellent stability at room temperature, with a variation of response current less than 5% over 30 days.

© 2011 Elsevier B.V. All rights reserved.

1. Introduction

The detection of hydrogen peroxide (H_2O_2) has become extremely important because of its wide and varied applications. As a well-known oxidizing agent, H_2O_2 is employed in textiles, cleaning products, organic compounds, the food industry, and for environmental treatments [1–3]. Several analytical methods have been developed to detect and quantify H_2O_2 , including spectrometry [4,5], titrimetry [6], chemiluminescence [7–9], and electrochemistry [10–12]. Among these, electrochemical methods have emerged as preferable due to their relatively low cost, efficiency, high sensitivity, and ease of operation.

Horseradish peroxidase, cytochrome C, hemoglobin, and myoglobin have been widely used to construct various amperometric biosensors for H_2O_2 detection due to their high sensitivity and selectivity [13–18]. However, there are several disadvantages of the enzyme-modified electrodes, such as instability, high cost of enzymes and complicated immobilization procedure. The activity of enzymes can be easily affected by temperature, pH value, and toxic chemicals. In order to solve these problems, considerable attention has been paid to develop nonenzymatic electrodes, for instance, noble metals, metal alloys, and metal nanoparticles [19–21]. However, these kinds of electrodes have displayed the drawbacks of low sensitivity, poor selectivity and high cost. There-

fore, the development of a cheap and highly sensitive catalyst for nonenzymatic H_2O_2 detection is still greatly demanded.

Flavin adenine dinucleotide (FAD) is a flavoprotein coenzyme that plays an important biological role in many oxidoreductases and in reversible redox conversions in biochemical reactions. It consists of the nucleotide adenine, the sugar ribose, and two phosphate groups. FAD and FADH_2 have an isoalloxazine ring as the redoxactive component that readily accepts and donates electrons. This makes it ideally suited to be an intermediate that is cyclically reduced and then re-oxidized by the metabolic reactions. The adsorption of FAD has been studied on Hg electrode [22], on the surface of titanium electrodes [23], and its electrochemical properties have been determined [24]. The electrocatalytic reduction for H_2O_2 was also found while FAD-modified zinc oxide self-assembly film was studied in the absence/presence of hemoglobin [25]. It is worthy to further investigate the electrocatalytic reduction of H_2O_2 with FAD and its hybrid composite.

Methylene blue (MB) or tetramethylthionine chloride is one of the basic dyes with the structure of heterocyclic aromatic chemical compound. The cationic dyes were commonly used initially for dyeing of silk, leather, plastics, paper, cotton mordanted with tannin, and also in manufacturing of paints and printing inks [26]. Due to this interaction capability, MB has been extensively used as redox marker in electrochemical biosensors to detect the hybridization event [27–31].

In this work, we report a simple method to immobilize methylene blue (MB) and FAD on electrode surface for electrocatalytic reduction of H_2O_2 . This hybrid film is synthesized

* Corresponding author. Tel.: +886 2 27017147; fax: +886 2 27025238.
E-mail address: smchen78@ms15.hinet.net (S.-M. Chen).

by electropolymerization of MB and static interaction between poly(methylene blue) (PMB) and FAD. It is further characterized and discussed in electrochemical behaviors, surface morphology, and electrocatalytic property by cyclic voltammetry, scanning electron microscopy, atomic force microscopy, and amperometry.

2. Materials and methods

2.1. Reagents and materials

Hydrogen peroxide (H_2O_2), flavin adenine dinucleotide (FAD), methylene blue (MB) monomer, potassium chlorate (KClO_3), potassium bromate (KBrO_3), potassium iodate (KIO_3), sodium hypochlorite (NaClO), nicotinamide adenine dinucleotide (NADH), were purchased from Sigma–Aldrich (USA). All other chemicals (Merck) used were of analytical grade (99%). Double distilled deionized water (DDDW) was used to prepare all the solutions. A phosphate buffer solution (PBS) of pH 7 was prepared using Na_2HPO_4 (0.05 mol L^{-1}) and NaH_2PO_4 (0.05 mol L^{-1}).

2.2. Apparatus

All electrochemical experiments were performed using CHI 1205a potentiostats (CH Instruments, USA). The BAS GCE (0.3 cm in diameter, exposed geometric surface area 0.07 cm^2 , Bioanalytical Systems, Inc., USA) was used. A conventional three-electrode system was used which consists of an Ag/AgCl (3 M KCl) as a reference electrode, a GCE as a working electrode, and platinum wire as a counter electrode. For the rest of the electrochemical studies, Ag/AgCl (3 M KCl) was used as a reference. The morphological characterization of composite films was examined by means of SEM (S-3000H, Hitachi) and AFM images were recorded with multimode scanning probe microscope (Being Nano-Instruments CSPM-4000, China). Indium tin oxide (ITO) glass was the substrate of different films for AFM analysis. The buffer solution was entirely altered by deaerating using nitrogen gas atmosphere. The electrochemical cells were kept properly sealed to avoid the oxygen interference from the atmosphere. All electrochemical experiments were performed under anaerobic condition to avoid the voltammetric response of oxygen reduction in the system.

2.3. Preparation of PMB/FAD hybrid films

Since PMB film can be easily formed on electrode surface by the MB electropolymerization, we plan to do the electro-codeposition of PMB and FAD hybrid films utilizing the electrostatic interaction between the positive charge PMB and the negative charge FAD. PMB/FAD hybrid films were prepared on GCE and ITO electrodes surface by repeatedly cyclic voltammetry. Fig. 1 shows the PMB/FAD film growth using GCE in PBS (pH 7) containing $1 \times 10^{-4} \text{ M}$ methylene blue and $1 \times 10^{-4} \text{ M}$ FAD. However, the FAD redox couple is obvious smaller than PMB in the cyclic voltammogram. In order to have the similar current height of these three redox couples to easily monitor the electrochemical behaviors of this hybrid film, we adjusted the higher FAD concentration in the prepared solution containing $1 \times 10^{-3} \text{ M}$ FAD and $2.5 \times 10^{-4} \text{ M}$ MB. These film modified electrodes were appropriately used to study in this work.

3. Results and discussion

3.1. Immobilization of PMB/FAD hybrid film on electrode surface

Poly(methylene blue) and FAD hybrid film can be performed on electrode surface using glassy carbon electrode in neutral aque-

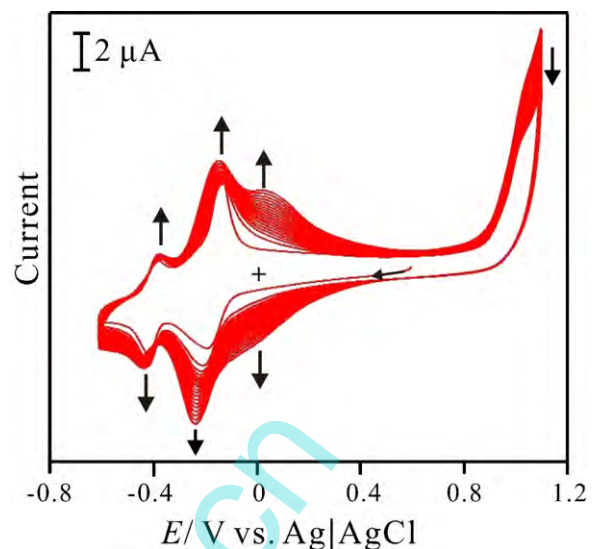


Fig. 1. Repeatedly cyclic voltammograms of electropolymerization for PMB/FAD hybrid film in 0.1 M PBS (pH 7) containing $1 \times 10^{-4} \text{ M}$ methylene blue and $1 \times 10^{-4} \text{ M}$ FAD, scan rate = 0.1 V s^{-1} .

ous solution. The hybrid film was briefly mentioned in PMB/FAD for convenience. Fig. 1 shows the voltammogram of PMB/FAD film growth which had three redox couples in PBS (pH 7) containing 10^{-4} M methylene blue and 10^{-4} M FAD. Two relatively positive redox couples with formal potential (E^0) of 0 V and -0.2 V are known for poly(methylene blue) (PMB) and methylene blue monomer [32], respectively. The relative negative one ($E^0 = -0.4 \text{ V}$) is known for FAD redox couple. From Fig. 1, the peak currents of PMB redox couples (the relatively positive two redox couples) were more obvious than that of FAD (the relatively negative redox couple) after 30 scanning cycles with the scan rate at 0.1 V s^{-1} . This is because PMB formation is potential dependent. FAD can be further immobilized by the electrostatic interaction between the negative phosphate of FAD and the positive charge of PMB. So, the peak current development of FAD redox couple is limited by the formed PMB on electrode surface. It would be getting hard to load FAD once PMB occupied by more and more FAD. Hence, one can conclude that the hybrid film was prepared by electropolymerization of methylene blue and electrostatic interaction between PMB and FAD resulted in PMB/FAD co-immobilized on the electrode surface. The deposition amounts of PMB and FAD were estimated by EQCM. After the EQCM experiment, the charge under anodic peak of FAD was calculated with the CV curve. From the charge, using Faradays laws, the mass of FAD was estimated. From the data obtained after the three cyclic voltammetric scans, the PMB and FAD amounts were estimated about 105 ng cm^{-2} of PMB and 35 ng cm^{-2} of FAD, respectively.

3.2. Electrochemical characteristics of PMB/FAD hybrid film

Fig. 2 shows the cyclic voltammograms of the resulting electrode obtained with various potential scan rates in 0.1 M PBS (pH 7). The electrochemical response of PMB/FAD exhibited redox peaks which attribute to the electron transformations between PMB and FAD in the hybrid film. The electrochemical properties of modified GC electrode with PMB/FAD were studied by cyclic voltammetry in pure buffered aqueous solution (pH 7) at various scan rates.

From Fig. 2, it shows the cyclic voltammograms of PMB/FAD/GCE at various scan rates ($10\text{--}500 \text{ mV s}^{-1}$). The peak currents of redox couples are directly proportional to scan rates up to 500 mV s^{-1} (Fig. 2C) as expected for surface confined process. As can be seen in

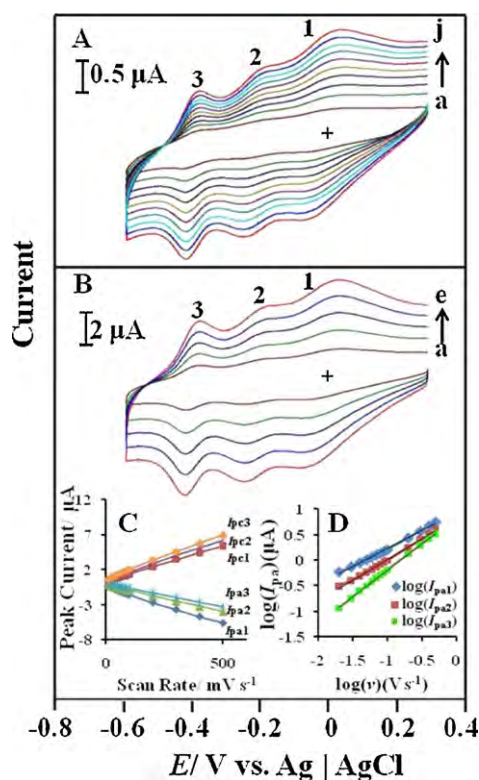


Fig. 2. Cyclic voltammograms of PMB/FAD/GCE examined in 0.1 M PBS (pH 7) with different scan rate of (A) low scan rate: (a) 0.01 V s⁻¹, (b) 0.02 V s⁻¹, (c) 0.03 V s⁻¹, (d) 0.04 V s⁻¹, (e) 0.05 V s⁻¹, (f) 0.06 V s⁻¹, (g) 0.07 V s⁻¹, (h) 0.08 V s⁻¹, (i) 0.09 V s⁻¹, and (j) 0.1 V s⁻¹; and (B) high scan rate: (a) 0.1 V s⁻¹, (b) 0.2 V s⁻¹, (c) 0.3 V s⁻¹, (d) 0.4 V s⁻¹, and (e) 0.5 V s⁻¹, respectively. (C) Plot of anodic and cathodic peak current (I_{pa} & I_{pc}) vs. scan rate. (D) Plot of logarithmic regressing equation of anodic peak current and scan rate.

Fig. 2D, the logarithmic regressing equation of anodic peak current and scan rate can be expressed as:

Anodic peak 1:

$$\log(I_{pa1}) = 0.7136 \log(\nu) + 0.9434 \quad (R^2 = 0.9963),$$

Anodic peak 2:

$$\log(I_{pa2}) = 0.803 \log(\nu) + 0.8168 \quad (R^2 = 0.9970), \text{ and}$$

Anodic peak 3:

$$\log(I_{pa3}) = 1.0321 \log(\nu) + 0.8365 \quad (R^2 = 0.9996), \text{ where } I_{pa} \text{ is anodic peak current in } \mu\text{A} \text{ and } \nu \text{ is scan rate in } \text{mV s}^{-1}.$$

Moreover, the ratio of oxidation-to-reduction peak current is nearly unity and formal potential is not change with increasing scan rate in this pH condition. This result reveals that the electron transfer kinetics is very fast on the electrode surface.

The results show that the PMB/FAD film was both stable and electrochemically active in the aqueous buffer solution. Fig. 2C shows a linear dependence between peak current and scan rate. The non-zero nature of these redox couples may be due to the reversible electron transfer process. The peak current and scan rate are related

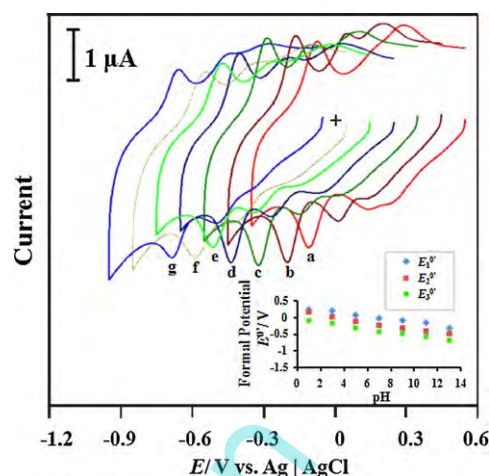


Fig. 3. Cyclic voltammograms of PMB/FAD/GCE examined in various pH conditions of: (a) pH 1, (b) pH 3, (c) pH 5, (d) pH 7, (e) pH 9, (f) pH 11, and (g) pH 13, respectively, scan rate = 0.1 V s⁻¹. Inset: plot of formal potential of PMB/FAD/GCE vs. pH (E_1^0 , E_2^0 and E_3^0 represent formal potential of three redox couples marked from positive to negative potential).

by the following relationship [33,34]:

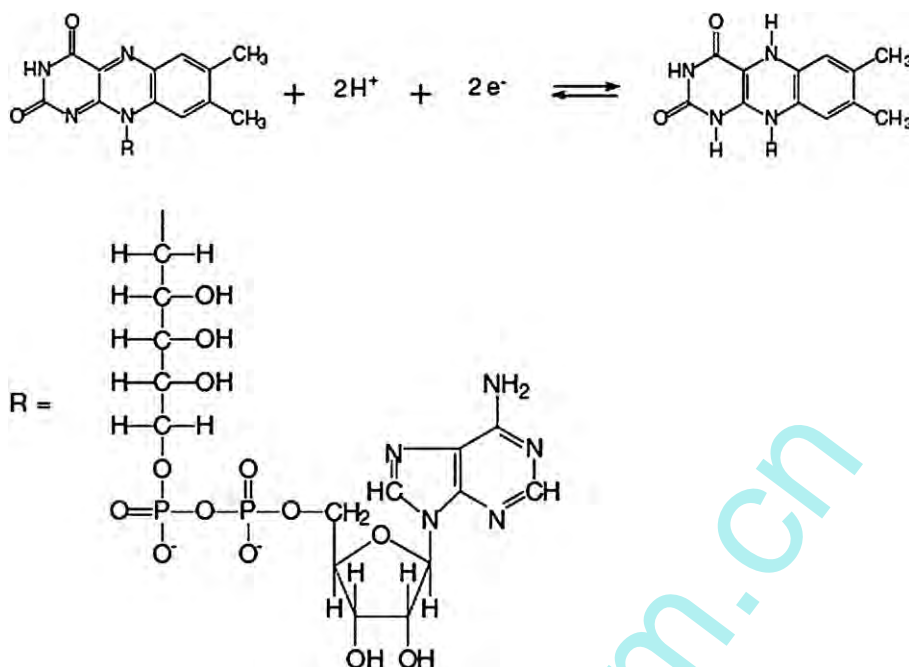
$$I_p = \frac{n^2 F^2 \nu A \Gamma_0}{4RT} \quad (1)$$

where, Γ_0 , ν , A , and I_p represent the surface coverage, the scan rate, the area of the electrode, and the peak current, respectively. The above relation shows that the behavior of the PMB/FAD hybrid film on a glassy carbon electrode surface is consistent with a diffusionless reversible electron transfer process.

Fig. 3 displays the pH-dependent voltammetric response of PMB/FAD modified electrode. In order to ascertain this, the voltammetric responses of PMB/FAD electrode were obtained in the solutions of different pH values varying from 1 to 13. As can be seen in Fig. 3, the three redox couples of PMB/FAD are pH dependent and their formal potential (E^0) will shift negatively as increasing pH value of the solution. This shows that the film is stable in the pH range between 1 and 13. The inset in Fig. 3 shows the formal potential (E_1^0 , E_2^0 , E_3^0) of PMB/FAD plotted over a pH range of 1–13. E_1^0 , E_2^0 and E_3^0 represent the formal potential of the three redox couples of PMB/FAD. They are marked by the potential order from the relatively positive to the relatively negative. The response of PMB redox couples (E_1^0 and E_2^0) shows a slope of -68 mV/pH (for pH 1–7) and -39 mV/pH (for pH 7–13), which is close to that given by the Nernstian equation [35] for equal (for pH 1–7) and non-equal (for pH 7–13) number of electrons and protons transfer processes. The response of FAD redox couple (E_3^0) shows a slope of -58 mV/pH (for pH 1–13) which is close to that expected from calculations using Nernstian equation. The phenomenon indicates that the number of electrons and protons is the same. In our case, two electrons and one proton were involved in the PMB redox couple [32], whereas two electrons and two protons were involved in the FAD redox couple [36]. Schemes 1 and 2 represent the reduction and oxidation states for methylene blue and FAD, respectively.



Scheme 1. The redox reaction of methylene blue.



Scheme 2. The redox reaction of FAD.

3.3. SEM and AFM analysis of PMB/FAD hybrid film

Scanning electron microscopy (SEM) and atomic force microscopy (AFM) were utilized to image the morphology of the active surface of the electrodeposited PMB films with/without FAD, and compared with the bare GCE or ITO, as shown in Fig. 4. The bare GCE appears flat surface, in contrast with the FAD, PMB, and PMB/FAD film modified GCE electrodes, which has a relatively smooth surface in SEM images (Fig. 4A–D). FAD (prepared by adsorption) exhibits specific circular shape might be due to the aggregation of FAD molecules. PMB (prepared by electropolymerization) has unique fiber-like structure might be due to the formation of polymer chain. Particularly, the PMB/FAD (co-immobilized by electropolymerization) shows much uniform structure than both FAD and PMB. Compared with the AFM images (Fig. 4A'–D') of these films, they have the same morphology similar to their respective SEM images. Average diameter of these films was found in 183.7 nm, 108.9 nm, and 47.9 nm for FAD, PMB, and PMB/FAD, respectively. And the average height was found in 57.6 nm, 71.6 nm, and 21.4 nm. By comparison, the PMB polymerized layer has much thicker and extremely rough surface in SEM image. Moreover, it is found that PMB/FAD shows the uniform and relative small structure than PMB and FAD. This is extremely like that the film formation of static interaction between PMB and FAD leads to form a much smooth and compact structure.

3.4. Electrocatalytic properties of PMB/FAD hybrid film

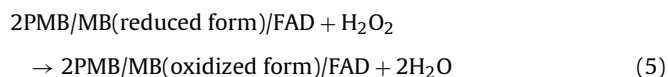
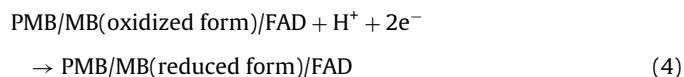
The electrocatalytic reduction of hydrogen peroxide, chlorate, bromate, iodate, and hypochlorite using the PMB/FAD hybrid film was investigated. Fig. 5A displays the electrocatalytic reduction cyclic voltammogram of hydrogen peroxide by PMB/FAD/GCE in pH 7 PBS solution. During scanning potential range from 0.4 to –0.6V, two cathodic peaks (at about –0.45V and –0.25V) were found obvious current increasing as additions of hydrogen peroxide. Compared with bare GCE electrode (a'), which shows almost no electrocatalytic current response for 4×10^{-4} M hydrogen peroxide in the same scanning potential range, this film modified electrode can show uniquely electrocatalytic potential and current. It means

that the PMB/FAD hybrid film can effectively lower over-potential of hydrogen peroxide and enhance the electrocatalytic current. This electrocatalytic mechanism can be expressed as following:

$$\text{At } E_{pc} = -0.45 \text{ V}$$



$$\text{At } E_{pc} = -0.25 \text{ V,}$$



Inset of Fig. 5A shows the plot of electrocatalytic peak current (I_p) versus H_2O_2 concentration. From the slope it exhibits the sensitivity of $5550 \mu\text{A M}^{-1}$ at $E_{pc} = -0.45$ V. As the examined results, PMB/FAD hybrid film can be a good choice to detect hydrogen peroxide especially for enzyme-free biosensor development. The sensitivity of this H_2O_2 biosensor will be fine estimated by amperometry in Section 3.5.

Fig. 5B displays the electrocatalytic reduction of hypochlorite using the PMB/FAD electrode in pH 7 PBS. Compared with bare GCE electrode (a'), which shows almost no electrocatalytic current response for 9×10^{-3} M hypochlorite in the same scanning potential range, the catalytic current was obviously increasing in three cathodic peaks (at about –0.45V, –0.25V, and –0.05V) as additions of hypochlorite. This electrocatalytic mechanism can be expressed as following:

$$\text{At } E_{pc} = -0.45 \text{ V,}$$



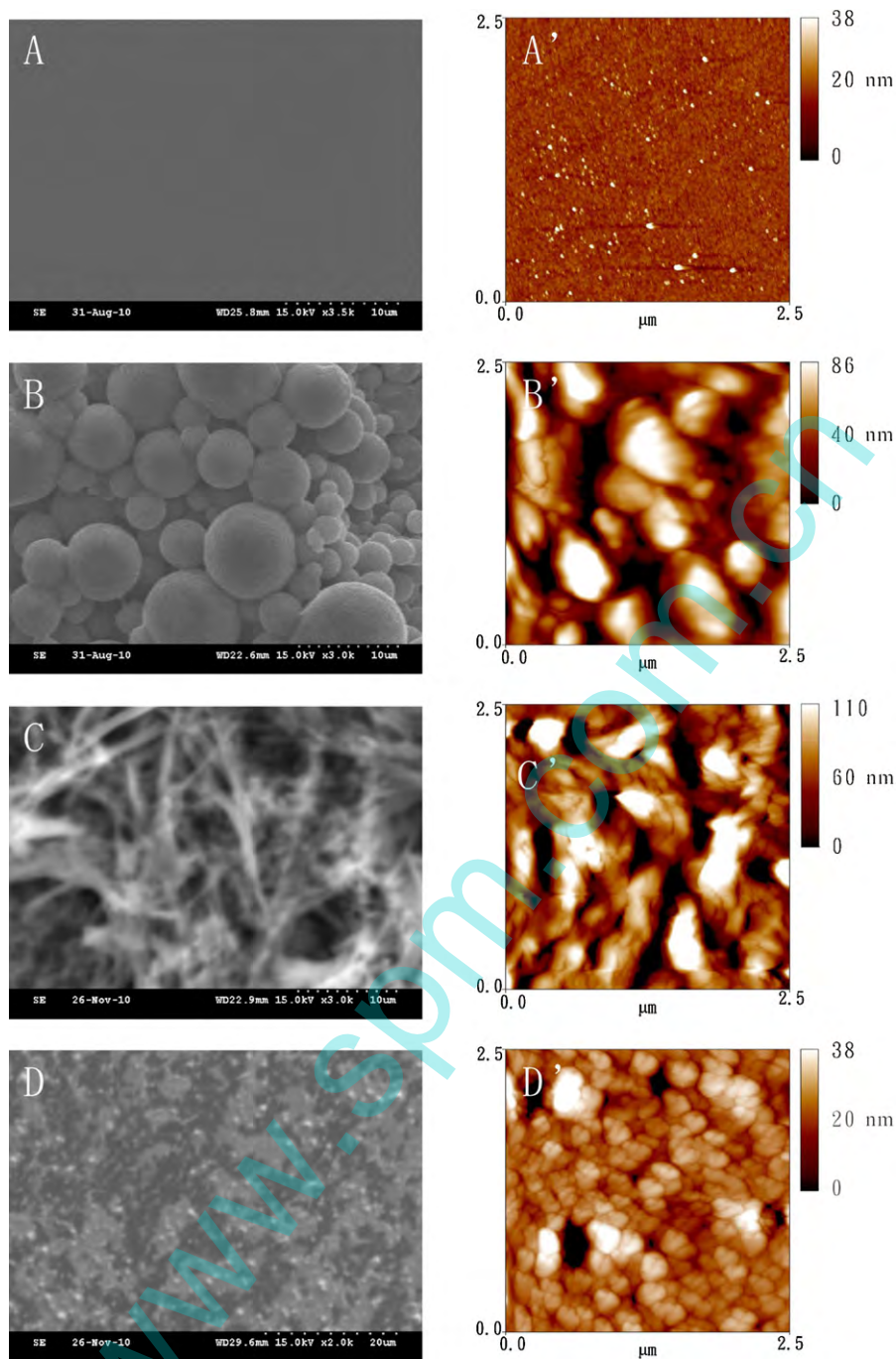
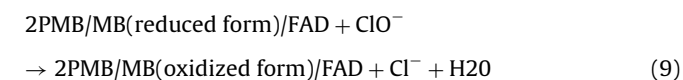
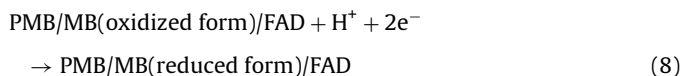
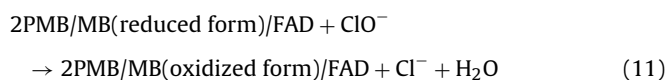
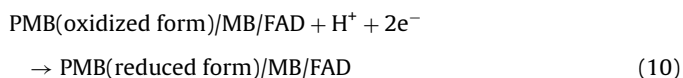


Fig. 4. SEM images of: (A) bare GCE, (B) FAD/GCE, (C) PMB/GCE and (D) PMB/FAD/GCE; tapping mode AFM images of (A') bare ITO, (B') FAD/ITO, (C') PMB/ITO and (D') PMB/FAD/ITO.

At $E_{pc} = -0.25$ V,



At $E_{pc} = -0.05$ V,



Inset of Fig. 5B shows the plot of electrocatalytic peak current (I_p) versus NaClO concentration. From the slope it exhibits the sensitivity of $95 \mu\text{A M}^{-1}$ at $E_{pc} = -0.45$ V. It was found that the PMB/FAD hybrid film was good electro-active species for hypochlorite.

The electrocatalytic reduction of the halates (chlorate, bromate, and iodate) using PMB/FAD hybrid film was also studied by cyclic voltammetry. Fig. 5C and D display the cyclic voltammograms of electrocatalytic reduction for bromate and iodate, respectively. The

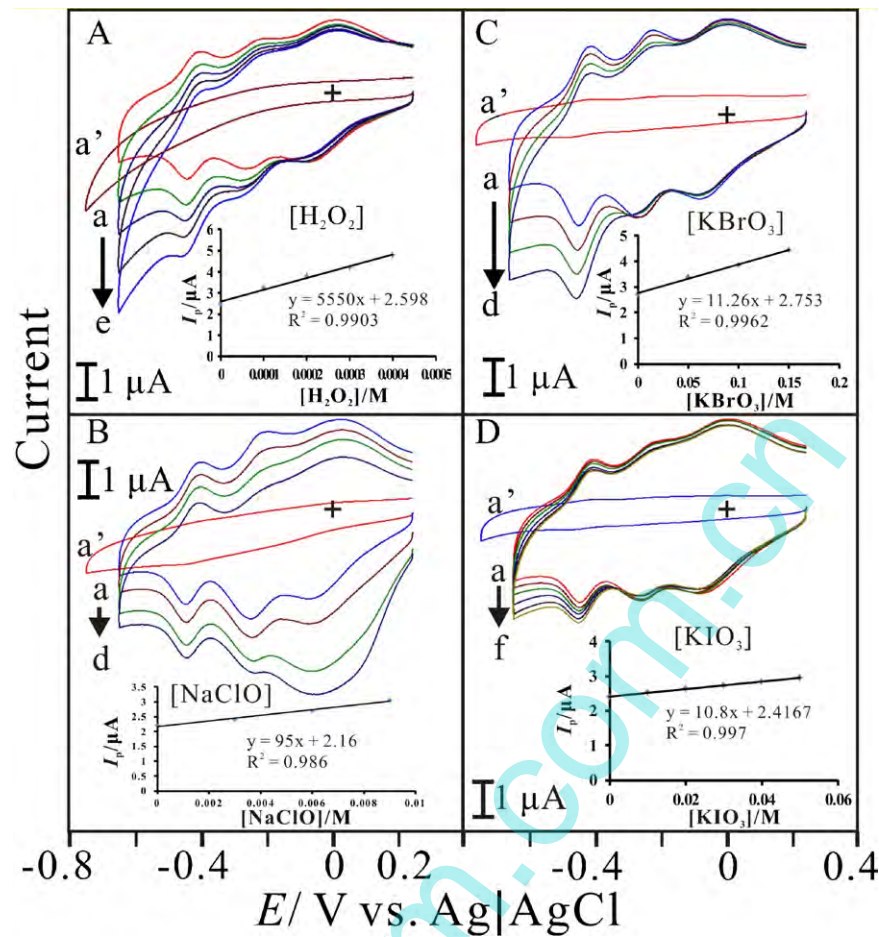


Fig. 5. Cyclic voltammograms of PMB/FAD/GCE examined in 0.1 M PBS (pH 7) or 0.1 M KHP (pH 4) in the presence of: (A) $[\text{H}_2\text{O}_2]$ =(a) 0 M, (b) 1×10^{-4} M, (c) 2×10^{-4} M, (d) 3×10^{-4} M, and (e) 4×10^{-4} M; (B) $[\text{NaClO}]$ =(a) 0 M, (b) 3×10^{-3} M, (c) 6×10^{-3} M, and (d) 9×10^{-3} M; (C) $[\text{KBrO}_3]$ =(a) 0 M, (b) 5×10^{-2} M, (c) 0.1 M, and (d) 0.15 M; (D) $[\text{KIO}_3]$ =(a) 0 M, (b) 1×10^{-2} M, (c) 2×10^{-2} M, (d) 3×10^{-2} M, (e) 4×10^{-2} M, and (f) 5×10^{-2} M, respectively; (a') is cyclic voltammogram of the bare GCE examined in the maximal concentration of reactants for each case (A–D), scan rate = 0.1 V s^{-1} . Insets: the plots of electrocatalytic peak current (I_p) vs. species concentration.

electrocatalytic mechanism can be expressed as following:



Insets of Fig. 5C and D show the plots of electrocatalytic peak current (I_p) versus KBrO_3 and KIO_3 concentration. From the slopes this sensor exhibits the sensitivity of $11.26 \mu\text{A M}^{-1}$ and $10.8 \mu\text{A M}^{-1}$ for KBrO_3 and KIO_3 , respectively. By the test result, it was found bromate and iodate could be electrocatalytic reduced by the hybrid film.

This hybrid film was further used to electrocatalytic oxidize NADH in PBS (pH 7). Fig. 6 displays the cyclic voltammogram of electrocatalytic oxidation for NADH. It was found anodic current increasing as additions of NADH while almost no current response was found at bare electrode. However, it was noticed that the electrocatalytic peak current seems not obvious at $E_{\text{pa}} = 0.05 \text{ V}$. It was found more obvious at $E_{\text{pa}} = 0.2 \text{ V}$. This might be due to the delay electron transformation between PMB polymer chain and NADH. From the result, it was understood that NADH was electrocatalytic oxidized by PMB redox couple. According to our experiment result, the reaction mechanism when using a PMB/FAD hybrid film as a catalyst can be described below:

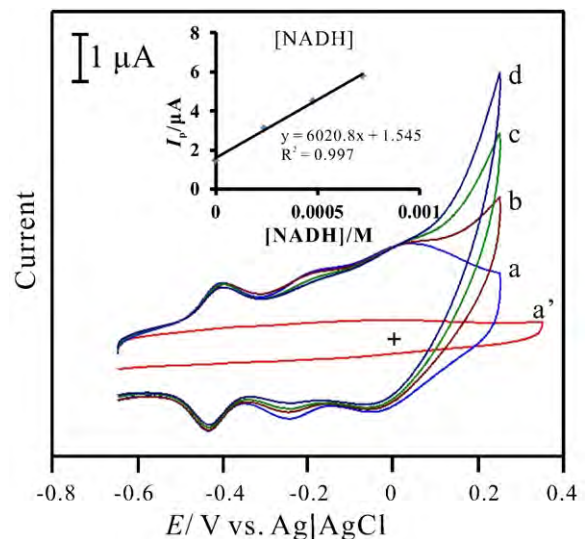
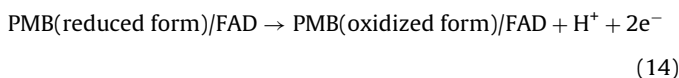
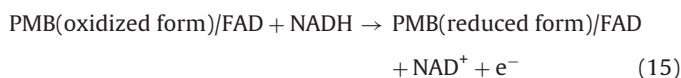


Fig. 6. Cyclic voltammograms of PMB/FAD/GCE examined in 0.1 M PBS (pH 7) in the presence of $[\text{NADH}]$ =(a) 0 M, (b) 2.4×10^{-4} M, (c) 4.8×10^{-4} M, and (d) 7.2×10^{-4} M, respectively; (a') is cyclic voltammogram of the bare GCE examined in the maximal concentration in this case, scan rate = 0.1 V s^{-1} . Inset: the plot of electrocatalytic peak current (I_p) versus NADH concentration.

Table 1

The electrocatalytic properties of poly(methylene blue)/FAD film with various reactants in PBS (pH 7).

Substrate	Electrocatalytic reaction type	Electrocatalytic peak potential (V) (vs. Ag/AgCl)
H ₂ O ₂	Reduction	−0.45, −0.25
NaClO	Reduction	−0.45, −0.25, −0.05
BrO ₃ [−]	Reduction	−0.45
IO ₃ [−]	Reduction	−0.45
NADH	Oxidation	0.20



Inset of Fig. 6 shows the plot of electrocatalytic peak current (I_p) versus NADH concentration. It exhibits the sensitivity of $6020.8 \mu\text{A M}^{-1}$ at $E_{pa} = 0.2 \text{ V}$.

As result shown in Table 1, we conclude that the PMB/FAD hybrid film is a good electroactive material due to good electrocatalytic reaction for hydrogen peroxide, hypochlorite, bromate, and iodate. Particularly, it might be developed one multi-functional sensor for these species. According to the sensitivity of these analytes (the insets of the new Fig. 5), the H₂O₂ sensitivity has about 50 times more than those of other analytes (hypochlorite, bromate, iodate) except of NADH. A simple, enzyme-free, and low costly hydrogen peroxide biosensor was studied in the next section.

3.5. Amperometric response of hydrogen peroxide electrocatalysis by PMB/FAD hybrid film

The determination of hydrogen peroxide using PMB/FAD electrode was studied by amperometry. Amperometric response with additions of hydrogen peroxide was tested to study electrocatalytic reduction of hydrogen peroxide by PMB/FAD film modified GCE electrode in the deaerating PBS solution. Fig. 7 shows amperometric response of hydrogen peroxide that was evaluated at PMB/FAD/GCE. Applied potential is set at -0.45 V with electrode rotation speed of 1000 rpm. Initial period of 0–200 s, amperometric response of PMB/FAD/GCE is tested for blank. As sequential additions of 10^{-4} M hydrogen peroxide per 50 s by micro-syringe during 200–5000s, the correlative amperometric response of PMB/FAD/GCE can be found. As tested result, PMB/FAD/GCE has detection limit of $0.1 \mu\text{M}$ and shows linearly amperometric responses for hydrogen peroxide in the concentration of $0.1\text{--}960 \mu\text{M}$. It has sensitivity of $1109 \mu\text{A mM}^{-1} \text{ cm}^{-2}$ and signal/noise of 3 as shown in Fig. 7. The relative standard deviation (RSD) for determining H₂O₂ ($n = 10$) was 2.87%. It indicates that the sensor has very good reproducibility at pH 7. As shown in

Table 2

Comparison of the performance of different enzyme-free H₂O₂ sensors.

Modifiers	Working potential (V) (vs. Ag/AgCl)	Linear range (μM)	LOD (μM)	Sensitivity ($\text{mA M}^{-1} \text{ cm}^{-2}$)	Ref.
Nanostructured Prussian Blue ^a	0.05	$10^{-3}\text{--}10^4$	0.001	700	[37]
Conventional (unstructured) Prussian Blue ^a	0.05	$10^{-1}\text{--}10^3$	0.001	500–700	[37]
Prussian Blue ^a	−0.05	$10^{-1}\text{--}10^2$	0.10	600	[38]
Cerium oxide nanoparticles ^a	0.2	1–50	1	15	[39]
Polymer/Pt nanoparticle ^b	0.6	$4.2 \times 10^{-2}\text{--}1.6 \times 10^2$	0.042	500	[40]
Pt nanowire ^a	0	$10^2\text{--}6 \times 10^4$	0.050	540	[41]
CNT/nano-Pt ^b	0.55	$2.5 \times 10^{-2}\text{--}2 \times 10^3$	0.025	3886	[42]
Carbon film/nano-Pt ^b	0.6	$5 \times 10^{-1}\text{--}2 \times 10^3$	0.0075	56	[43]
Ensembles of nano-Pt ^b	0.5	$5 \times 10^{-4}\text{--}4 \times 10^3$	500	21	[44]
PMB/FAD ^a	−0.45	$10^{-1}\text{--}9.6 \times 10^2$	0.10	1109	This work

^a Sensing of H₂O₂ by its reduction.

^b Sensing of H₂O₂ by its oxidation.

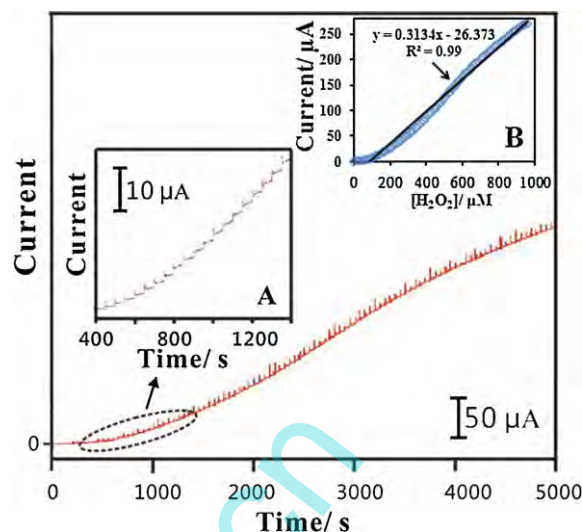


Fig. 7. Amperometric responses of sequential additions of H₂O₂ (10^{-6} M per time) tested by PMB/FAD/GCE in 0.1 M PBS (pH 7) solution, rotating speed = 1000 rpm, $E_{app} = -0.45 \text{ V}$ (insets: (A) scale-up amperomograms of PMB-FAD/GCE during 400–1200 s; and (B) plot of current response vs. H₂O₂ concentration).

Table 2, this electrode shows competitive sensitivity as compared with other enzyme-free (without HRP) H₂O₂ sensors. Having above information, it is good for developing hydrogen peroxide sensor.

3.6. Stability study of PMB/FAD hybrid film

Repetitive redox cycling experiments were done to determine the extent of stability relevant to PMB/FAD modified GCE in 0.1 M PBS solution (pH 7). This investigation indicated that after 100 continuous scan cycles with scan rate of 0.1 V s^{-1} , the peak heights of the cyclic voltammograms decreased less than 5%. On the other hand, the PMB/FAD modified GCE kept its initiate activity for more than one month as kept in 0.1 M PBS solution (pH 7). A decrease of 8% was observed in current response of the electrode at the end of 30th day. And the electrocatalytic response current of PMB/FAD for H₂O₂, NADH, KBrO₃, KIO₃, and NaClO can keep more than 90% of original current response. The analytical applicability of the biosensor was evaluated by determining the recoveries of five H₂O₂ samples with different concentrations by the standard addition method. The results were satisfactory, with an average of 99.2%, as listed in Table 3. Based on above result, we suggest that this sensor could be a re-usable one due to its good stability and multi-functional property.

Table 3

H₂O₂ recoveries at various concentrations determined with the biosensor (PMB/FAD).

[H ₂ O ₂] (μM)	[H ₂ O ₂] Found ^a (μM)	Recovery (%)
1	1.01	101.0
1.5	1.49	99.3
2	1.97	98.5
2.5	2.48	99.2
5	4.89	97.8

^a Average of three measurements.

4. Conclusions

Here we report a method to form an enzyme-free H₂O₂ biosensor based on PMB/FAD nanocomposite. It has good electrocatalytic reduction for hydrogen peroxide without HRP enzyme and shows lower over-potential and higher current response as compared with bare electrode. Amperometric response of PMB/FAD/GCE is linearly dependent on H₂O₂ concentration. The proposed film also shows good electrocatalytic reaction for NADH, KBrO₃, KIO₃, and NaClO, respectively. It can be further utilized to develop multifunctional biosensors. As the results, the proposed method has excellent advantages of enzyme-free, multifunction, low cost, low over-potential, and high sensitivity.

Acknowledgement

This work was supported by the National Science Council of Taiwan (ROC).

References

- [1] Y. Usui, K. Sato, M. Tanaka, Catalytic dihydroxylation of olefins with hydrogen peroxide: an organic-solvent- and metal-free system, *Angew. Chem. Int. Ed.* 42 (2003) 5623–5625.
- [2] M.I. Prodromidis, M.I. Karayannis, Enzyme-based amperometric biosensors for food analysis. A review, *Electroanalysis* 14 (2002) 241–261.
- [3] D.J. Barrington, A. Ghadouani, Application of hydrogen peroxide for the removal of toxic cyanobacteria and other phytoplankton from wastewater, *Environ. Sci. Technol.* 42 (2008) 8916–8921.
- [4] C.P. Rinsland, P.F. Coheur, H. Herbin, C. Clerbaux, C. Boone, P. Bernath, L.S. Chiou, Detection of elevated tropospheric H₂O₂ (hydrogen peroxide) mixing ratios in ACE (Atmospheric Chemistry Experiment) subtropical infrared solar occultation spectra, *J. Quant. Spectrosc. Radiat. Transfer* 107 (2007) 340–348.
- [5] K.F. Fernandes, C.S. Lima, F.M.L. Lopes, C.H. Collins, Hydrogen peroxide detection system consisting of chemically immobilised peroxidase and spectrometer, *Process Biochem.* 40 (2005) 3441–3445.
- [6] A. Brestovisky, E. KirowaEisner, J. Osteryoung, Direct and titrimetric determination of hydrogen peroxide by reverse pulse polarography, *Anal. Chem.* 55 (1983) 2063–2066.
- [7] N. Yamashiro, S. Uchida, Y. Satoh, Y. Morishima, H. Yokoyama, T. Satoh, J. Sugama, R. Yamada, Determination of hydrogen peroxide in water by chemiluminescence detection: (I) Flow injection type hydrogen peroxide detection system, *J. Nucl. Sci. Technol.* 41 (2004) 890–897.
- [8] D. Janasek, U. Spohn, An enzyme-modified chemiluminescence detector for hydrogen peroxide and oxidase substrates, *Sens. Actuators B* 39 (1997) 291–294.
- [9] R. Pehrman, M. Amme, C. Cachoir, Comparison of chemiluminescence methods for analysis of hydrogen peroxide and hydroxyl radicals, *Czech. J. Phys.* 56 (2006) D373–D379.
- [10] M.W. Shao, Y.Y. Shan, N.B. Wong, S.T. Lee, Silicon nanowire sensors for bio-analytical application: glucose and hydrogen peroxide detection, *Adv. Funct. Mater.* 15 (2005) 1478–1482.
- [11] Y. Qiao, G. Yang, F. Jian, Y. Qin, L. Yang, Hydrogen peroxide electrochemical detection for the development of protein film-modified sensor, *Sens. Actuators B* 141 (2009) 205–209.
- [12] Y. Shen, M. Trauble, G. Wittstock, Detection of hydrogen peroxide produced during electrochemical oxygen reduction using scanning electrochemical microscopy, *Anal. Chem.* 80 (2008) 750–759.
- [13] L.M. Li, S.J. Xu, Z.F. Du, Y.F. Gao, J.H. Li, T.H. Wang, Electrografted poly(N-mercaptopethyl acrylamide) and Au nanoparticles-based organic/inorganic film: a platform for the high-performance electrochemical biosensors, *Chem. Asian J.* 5 (2010) 919–924.
- [14] X.B. Lu, J.H. Zhou, W. Lu, Q. Liu, J.H. Li, Carbon nanofiber-based composites for the construction of mediator-free biosensors, *Biosens. Bioelectron.* 23 (2008) 1236–1243.
- [15] C.H. Wang, C. Yang, Y.Y. Song, W. Gao, X.H. Xia, Adsorption and direct electron transfer from hemoglobin into a three-dimensionally ordered macroporous gold film, *Adv. Funct. Mater.* 15 (2005) 1267–1275.
- [16] L. Zhang, Direct electrochemistry of cytochrome c at ordered macroporous active carbon electrode, *Biosens. Bioelectron.* 23 (2008) 1610–1615.
- [17] H.Y. Liu, J.F. Rusling, N.F. Hu, Electroactive core-shell nanocluster films of heme proteins, polyelectrolytes, and silica nanoparticles, *Langmuir* 20 (2004) 10700–10705.
- [18] X. Kang, J. Wang, Z. Tang, H. Wu, Y.H. Lin, Direct electrochemistry and electrocatalysis of horseradish peroxidase immobilized in hybrid organic-inorganic film of chitosan/sol-gel/carbon nanotubes, *Talanta* 78 (2009) 120–125.
- [19] Y.Y. Song, D. Zhang, X.H. Xia, Nonenzymatic glucose detection by using a three-dimensionally ordered, macroporous platinum template, *Chem. Eur. J.* 11 (2005) 2177–2182.
- [20] J.J. Yu, J.R. Ma, F.Q. Zhao, B.Z. Zeng, Development of amperometric glucose biosensor through immobilizing enzyme in a Pt nanoparticles/mesoporous carbon matrix, *Talanta* 74 (2008) 1586–1591.
- [21] H.F. Cui, J.S. Ye, W.D. Zhang, C.M. Li, J.H.T. Luong, F.S. Sheu, Selective and sensitive electrochemical detection of glucose in neutral solution using platinum-lead alloy nanoparticle/carbon nanotube nanocomposites, *Anal. Chim. Acta* 594 (2007) 175–183.
- [22] V.I. Birss, S. Guha-Thakurta, C.E. McGarvey, S. Quach, P. Vanysek, Adsorbed lumiflavin at mercury electrode surfaces, *J. Electroanal. Chem.* 456 (1998) 71–82.
- [23] R. Garjonyte, A. Malinauskas, L. Gorton, Investigation of electrochemical properties of FMN and FAD adsorbed on titanium electrode, *Bioelectrochemistry* 61 (2003) 39–49.
- [24] Y. Wang, G. Zhu, E. Wang, Electrochemical behavior of FAD at a gold electrode studied by electrochemical quartz crystal microbalance, *Anal. Chim. Acta* 338 (1997) 97–101.
- [25] K.C. Lin, S.M. Chen, The electrochemical preparation of FAD/ZnO with hemoglobin film-modified electrodes and their electroanalytical properties, *Biosens. Bioelectron.* 21 (2006) 1737–1745.
- [26] H. Berneth, A.G. Bayer, Ullmann's Encyclopedia of Industrial Chemistry, Wiley-VCH Press, Germany, 2003, pp. 585.
- [27] P. Kara, K. Kerman, D. Ozkan, B. Meric, A. Erdem, Z. Ozkan, M. Ozsoz, Electrochemical genosensor for the detection of interaction between methylene blue and DNA, *Electrochem. Commun.* 4 (2002) 705–709.
- [28] D. Ozkan, P. Kara, K. Kerman, B. Meric, A. Erdem, F. Jelen, P.E. Nielsen, M. Ozsoz, DNA and PNA sensing on mercury and carbon electrodes by using methylene blue as an electrochemical label, *Bioelectrochemistry* 58 (2002) 119–126.
- [29] B. Meric, K. Kerman, D. Ozkan, P. Kara, S. Erensoy, U.S. Akarca, M. Mascini, M. Ozsoz, Electrochemical DNA biosensor for the detection of TT and Hepatitis B virus from PCR amplified real samples by using methylene blue, *Talanta* 56 (2002) 837–846.
- [30] K. Kerman, D. Ozkan, P. Kara, B. Meric, J.J. Gooding, M. Ozsoz, Voltammetric determination of DNA hybridization using methylene blue and self-assembled alkanethiol monolayer on gold electrodes, *Anal. Chim. Acta* 462 (2002) 39–47.
- [31] N. Zhu, A. Zhang, Q. Wang, P. He, Y. Fang, Electrochemical detection of DNA hybridization using methylene blue and electro-deposited zirconia thin films on gold electrodes, *Anal. Chim. Acta* 510 (2004) 163–168.
- [32] A.A. Karyakin, A.K. Strakhova, E.E. Karyakina, S.D. Varfolomeyev, A.K. Yatslirsky, The electrochemical polymerization of methylene blue and bio-electrochemical activity of the resulting film, *Synth. Metals* 60 (1993) 289–292.
- [33] A.J. Bard, L.R. Faulkner, *Electrochemical Method Fundamentals and Applications*, Wiley, New York, 1980.
- [34] A.P. Brown, F.C. Anson, Cyclic and differential pulse voltammetric behavior of reactants confined to the electrode surface, *Anal. Chem.* 49 (1977) 1589–1595.
- [35] T. Komura, G.Y. Niu, T. Yamaguchi, M. Asano, A. Matsuda, Coupled electron-proton transport in electropolymerized methylene blue and the influences of its protonation level on the rate of electron exchange with β-nicotinamide adenine dinucleotide, *Electroanalysis* 16 (2004) 1791–1800.
- [36] U. Yogeswaran, S.M. Chen, Multi-walled carbon nanotubes with poly(methylene blue) composite film for the enhancement and separation of electroanalytical responses of catecholamine and ascorbic acid, *Sens. Actuators B: Chem.* 130 (2008) 739–749.
- [37] A.K. Arkady, A.P. Elena, A.B. Ivan, E.K. Elena, Electrochemical sensor with record performance characteristics, *Angew. Chem.* 119 (2007) 7822–7824.
- [38] A.K. Arkady, E.K. Elena, Prussian Blue-based 'artificial peroxidase' as a transducer for hydrogen peroxide detection. Application to biosensors, *Sens. Actuators B: Chem.* 57 (1999) 268–273.
- [39] A. Mehta, P. Swanand, B. Hyungseok, J.C. Hyoung, S. Sudipta, A novel multivalent nanomaterial based hydrogen peroxide sensor, *Sens. Actuators A: Phys.* 134 (2007) 146–151.
- [40] P. Karam, L.I. Halaoui, Sensing of H₂O₂ at low surface density assemblies of Pt nanoparticles in polyelectrolyte, *Anal. Chem.* 80 (2008) 5441–5448.
- [41] M. Yang, F. Qu, Y. Lu, Y. He, G. Shen, R. Yu, Platinum nanowire nanoelectrode array for the fabrication of biosensors, *Biomaterials* 27 (2006) 5944–5950.
- [42] K.B. Male, S. Hrapovic, J.H.T. Luong, Electrochemically-assisted deposition of oxides on platinum nanoparticle/multi-walled carbon nanotube-modified electrodes, *Analyst* 132 (2007) 1254–1261.
- [43] T. You, O. Niwa, M. Tomita, S. Hirono, Characterization of platinum nanoparticle-embedded carbon film electrode and its detection of hydrogen peroxide, *Anal. Chem.* 75 (2003) 2080–2085.

- [44] C. Sudip, R.C. Retna, Pt nanoparticle-based highly sensitive platform for the enzyme-free amperometric sensing of H_2O_2 , *Biosens. Bioelectron.* 24 (2009) 3264–3268.

Biographies

Kuo-Chiang Lin received his Ph.D. in the Department of Chemical Engineering and Biotechnology, National Taipei University of Technology (NTUT), Taiwan in 2005. He was employed as a senior RD engineer in Young Optics Co., Taiwan from 2005 to 2009. Currently he is a postdoctoral fellow in the Department of Chemical Engineering and Biotechnology, NTUT, Taiwan. His research interests are in bio-electrochemistry, chemical sensors, biosensors, electrocatalysis and electroanalysis, photoelectrochemistry, dye-sensitized solar cell and photovoltaic cells.

Chien-Yu Yin is currently in her second year of study for a M.S. with the Electro-analysis and Bioelectrochemistry Group in National Taipei University of Technology (NTUT), Taiwan. Her current research is mainly focused on electrochemical sensors.

Shen-Ming Chen is a professor in the Department of Chemical Engineering and Biotechnology, National Taipei University of Technology, Taiwan since 1997. Dr. Shen-Ming Chen obtained his Ph.D. in the Department of Chemistry, National Taiwan University, Taiwan in 1990 and also persuaded as a visiting postdoctoral fellow in Institute of Inorganic Chemistry, University of Erlangen-Nuremberg, Germany in 1997. His research interests are based on the designing of various electrochemical and analytical devices such as biosensors and chemical sensors, sensors based on nano materials and the development of different kinds of electroanalytical methods and its application in biochemical and new analytical systems. Not only limited to this, he also interested in fuel cells and photovoltaic cells development.

www.spm.com.cn